

Differing roles of CD1d2 and CD1d1 proteins in type I natural killer T cell development and function

Sundararaj, Srinivasan; Zhang, Jingjing; Krovi, S Harsha; Bedel, Romain; Tuttle, Kathryn D; Veerapen, Natacha; Besra, Gurdyal S; Khandokar, Yogesh; Praveena, T; Le Nours, Jérôme; Matsuda, Jennifer L; Rossjohn, Jamie; Gapin, Laurent

DOI:

[10.1073/pnas.1716669115](https://doi.org/10.1073/pnas.1716669115)

License:

Other (please specify with Rights Statement)

Document Version

Peer reviewed version

Citation for published version (Harvard):

Sundararaj, S, Zhang, J, Krovi, SH, Bedel, R, Tuttle, KD, Veerapen, N, Besra, GS, Khandokar, Y, Praveena, T, Le Nours, J, Matsuda, JL, Rossjohn, J & Gapin, L 2018, 'Differing roles of CD1d2 and CD1d1 proteins in type I natural killer T cell development and function', *National Academy of Sciences. Proceedings*.
<https://doi.org/10.1073/pnas.1716669115>

[Link to publication on Research at Birmingham portal](#)

Publisher Rights Statement:

Differing roles of CD1d2 and CD1d1 proteins in type I natural killer T cell development and function, Srinivasan Sundararaj, Jingjing Zhang, S. Harsha Krovi, Romain Bedel, Kathryn D. Tuttle, Natacha Veerapen, Gurdyal S. Besra, Yogesh Khandokar, T. Praveena, Jérôme Le Nours, Jennifer L. Matsuda, Jamie Rossjohn, Laurent Gapin, *Proceedings of the National Academy of Sciences* Jan 2018, 201716669; DOI: 10.1073/pnas.1716669115

Published under the PNAS license (<http://www.pnas.org/page/authors/licenses>)

General rights

Unless a licence is specified above, all rights (including copyright and moral rights) in this document are retained by the authors and/or the copyright holders. The express permission of the copyright holder must be obtained for any use of this material other than for purposes permitted by law.

- Users may freely distribute the URL that is used to identify this publication.
- Users may download and/or print one copy of the publication from the University of Birmingham research portal for the purpose of private study or non-commercial research.
- User may use extracts from the document in line with the concept of 'fair dealing' under the Copyright, Designs and Patents Act 1988 (?)
- Users may not further distribute the material nor use it for the purposes of commercial gain.

Where a licence is displayed above, please note the terms and conditions of the licence govern your use of this document.

When citing, please reference the published version.

Take down policy

While the University of Birmingham exercises care and attention in making items available there are rare occasions when an item has been uploaded in error or has been deemed to be commercially or otherwise sensitive.

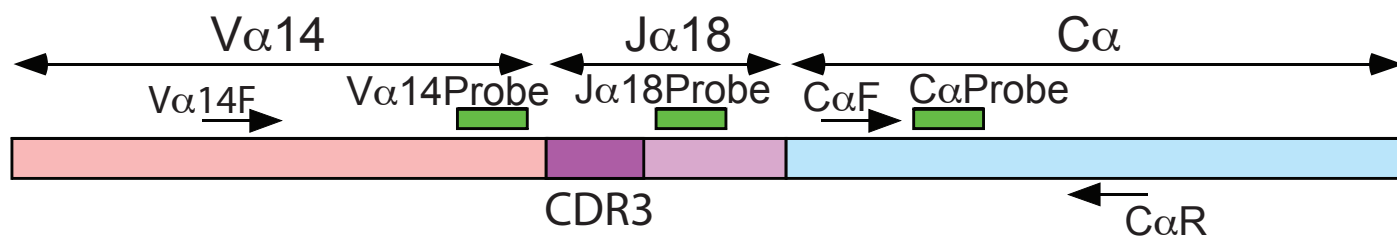
If you believe that this is the case for this document, please contact UBIRA@lists.bham.ac.uk providing details and we will remove access to the work immediately and investigate.

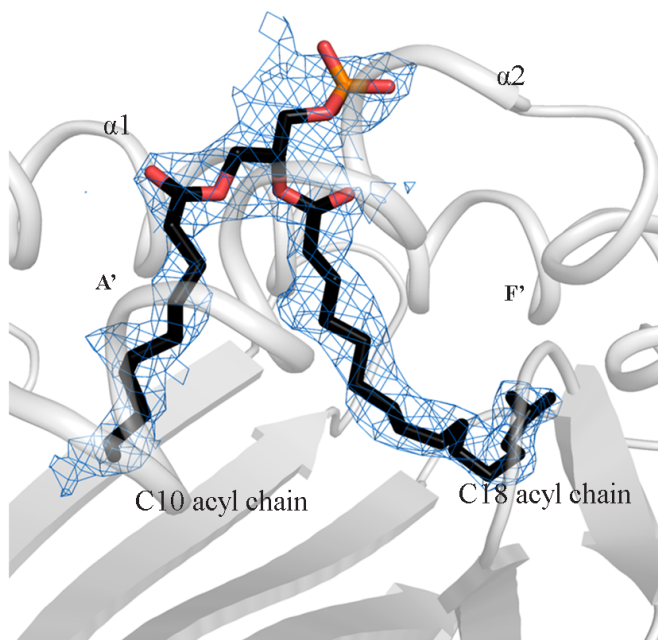
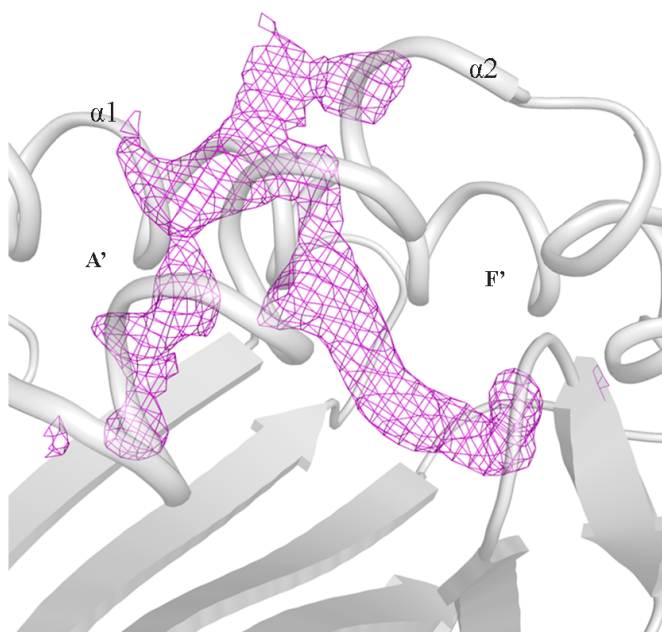
Supplementary Figure 1. The strategy used for the quantitative PCR is shown. V α 14 rearrangements were amplified with primers specific for V α 14 (V α 14F) and C α (C α R) and a V α 14-specific probe (V α 14Probe). Determination of J α 18-usage within V α 14 rearrangement was revealed using an identical amplification strategy (V α 14F-C α R) and a J α 18-specific probe (J α 18 Probe). In parallel, total amount of TCR rearrangements in each sample was determined by amplifying the TCR α constant region using specific primers and probe (C α F, C α R and C α Probe). The relative amount of V α 14 rearrangement was normalized to the amount of TCR α rearrangement in each sample. The relative J α 18 usage within V α 14 rearrangement was normalized to the total amount of V α 14 rearrangement in each sample.

Supplementary Figure 2. Left panel, unbiased Fo-Fc electron density map (in magenta) contoured at 2.2 σ level of the unknown endogenous bound lipid(s). Right panel, 2Fo-Fc electron density map (in marine) contoured at 0.8 σ level of the phosphatidic acid (C10) lipid Ag modeled in the unbiased electron density (Left panel). The lipid Ag is shown as black sticks. For clarity, only the α 1- and α 2- helices of CD1d2 are colored in light grey and shown as cartoon representation.

Supplementary Figure 3. Sequence alignment of *CD1D2* and *CD1D1*. The residues on a red background are strictly conserved whilst residues in red font and framed in blue are similar across both sequences. The secondary structural elements of CD1d2 are indicated atop the alignment and the numbering is based on the coordinates of the CD1d2 crystal structure. The alignment was computed using Clustal Omega (63) and edited by ESPrpt 3.0 (64).

Supplementary Figure 4. (A) Molecular surface of CD1d2 (in grey) and position of the non-conserved residues in CD1d1 (In magenta). (B) Molecular surface of the antigen-binding cleft of CD1d2 and footprint of the residues that form the cleft and that are not conserved in CD1d1 (in red).





mCD1d2 $\xrightarrow{\beta 1}$ $\xrightarrow{\beta 2}$ $\xrightarrow{\beta 3}$
 1 10 20 30 40 50
mCD1d2 SEAQQKNYTFRCLO^TSSFAN^HSWSR^TDS^LI^LLGDLQTHRWSNDSA^IISFT
mCD1d1 SEAQQKNYTFRCLO^MSSFAN^RSWSR^TDS^VW^LLGDLQTHRWSNDSA^TISFT

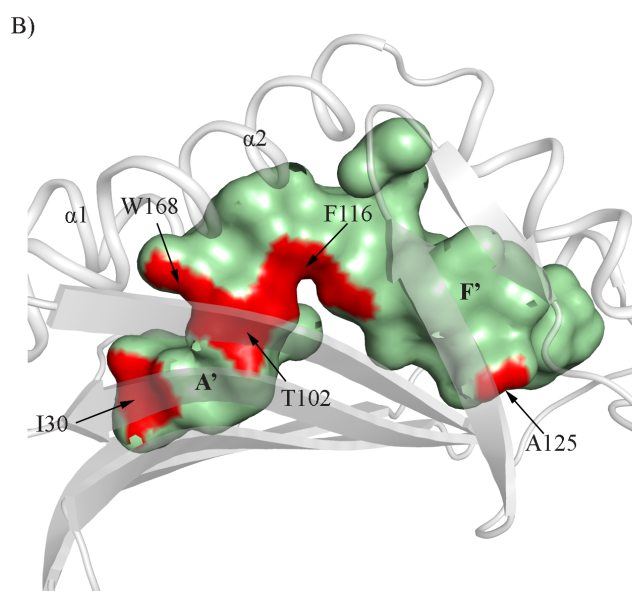
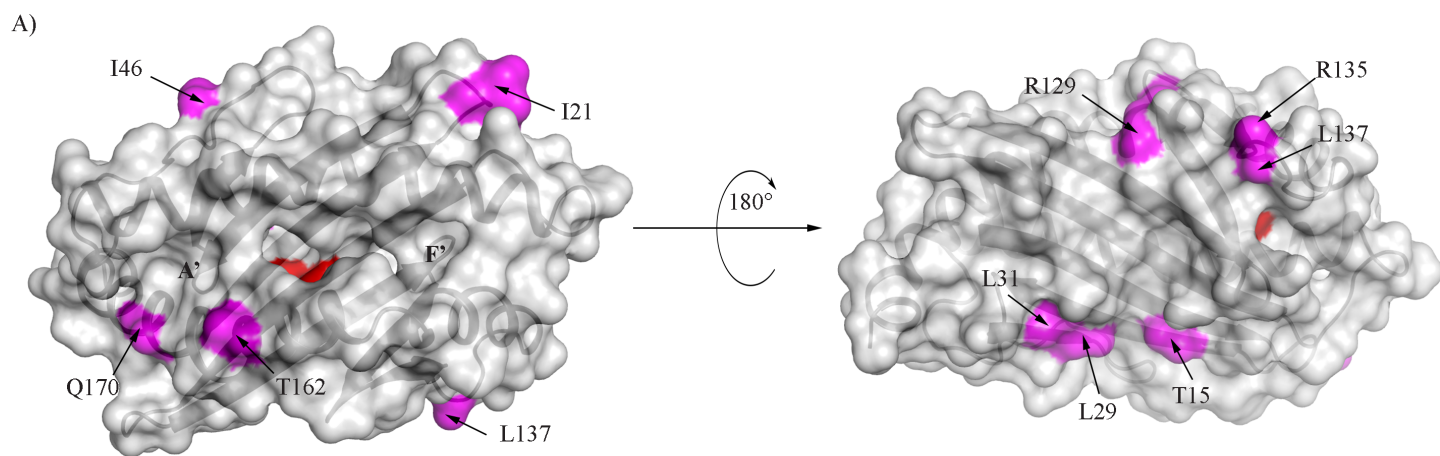
mCD1d2 $\xrightarrow{\alpha 1}$
 60 70 80 90 100
mCD1d2 KPWSQGKLSNQQWEKLOHMFQVYRVSFTRDIQELVKMMSPKEDYPIEIQ^L
mCD1d1 KPWSQGKLSNQQWEKLOHMFQVYRVSFTRDIQELVKMMSPKEDYPIEIQ^L

mCD1d2 $\xrightarrow{\beta 4}$ $\xrightarrow{\beta 5}$ $\xrightarrow{\beta 6}$ $\xrightarrow{\beta 7}$ $\xrightarrow{\alpha 2}$
 110 120 130 140 150
mCD1d2 S^TGC^EMYPGNASES^FF^HVAFQ^GKY^VVRF^RGT^SW^CR^VL^LGAPSWLDLPIKVL
mCD1d1 S^AGC^EMYPGNASES^FL^HVAFQ^GKY^VVRF^WGT^SW^CT^VL^LGAPSWLDLPIKVL

mCD1d2 $\xrightarrow{\alpha 2}$ $\xrightarrow{\beta 8}$
 160 170 180 190 200
mCD1d2 NADQ^GTSATV^CLLND^TW^PQ^FARGLLEAGKSDLEKQEK^PVAWLSSVPSSA
mCD1d1 NADQ^GTSATV^MLLND^TC^PL^FARGLLEAGKSDLEKQEK^PVAWLSSVPSSA

mCD1d2 $\xrightarrow{\beta 9}$ $\xrightarrow{\beta 10}$ $\xrightarrow{\beta 11}$ $\xrightarrow{\beta 12}$ $\xrightarrow{\beta 13}$ $\xrightarrow{\beta 14}$
 210 220 230 240 250
mCD1d2 H^GH^LQLVCHVSGFY^FPKPVVWMMRGDQEQ^GGTHRGD^FLPNADET^WYLQAT
mCD1d1 D^GH^RQLVCHVSGFY^FPKPVVWMMRGDQEQ^GGTHRGD^FLPNADET^WYLQAT

mCD1d2 $\xrightarrow{\beta 15}$ $\xrightarrow{\beta 16}$
 260 270 280
mCD1d2 LDVEAGEEAGLACRVKHSSLG^GQDI^ILYWDARQAPVG
mCD1d1 LDVEAGEEAGLACRVKHSSLG^GQDI^ILYWDARQAPVG



Supplementary table 1

Data collection and refinement statistics

	CD1d2-endogenous lipids	CD1d2- α -GalCer (C10)
Data collection		
Temperature	100K	100K
Resolution limits (Å)	46.19-2.43 (2.56-2.43)	45.93 -2.3 (2.38-2.30)
Space Group	$P2_1$	$P2_1$
Cell dimensions (Å)	$a=58.57$, $b=71.55$, $c=104.75$ $\beta=101.8$	$a=105.96$, $b=74.23$, $c=117.60$, $\beta=102.94^\circ$
Total N ^o . observations	239689 (34156)	556347 (30235)
N ^o . unique observations	32094 (4600)	79496 (7814)
Multiplicity	7.5 (7.4)	7.0 (6.9)
Data completeness	99.7 (98.4)	99.8 (97.5)
Wilson B-factors (Å ²)	50.3	36.19
I/ σ_I	17.9 (2.9)	11.6 (2.8)
R _{p.i.m} ¹ (%)	4.4 (31.2)	4.3 (34.8)
Refinement statistics		
R _{factor} ² (%)	21.5	23
R _{free} ³ (%)	25.1	28
Non hydrogen atoms		
- Protein	5836	11728
- Water	64	305
- Heterogen	84	363
Ramachandran plot (%)		
- Most favoured	97.6	98
- Allowed	2.4	2
r.m.s.d bonds (Å)	0.01	0.005
r.m.s.d angles (°)	1.11	0.83

¹ $R_{p.i.m} = \sum_{hkl} [1/(N-1)]^{1/2} \sum_i |I_{hkl,i} - \langle I_{hkl} \rangle| / \sum_{hkl} \langle I_{hkl} \rangle$

² $R_{factor} = (\sum ||F_o| - |F_c||) / (\sum |F_o|)$ - for all data except as indicated in footnote 3.

³ 5% of data was used for the R_{free} calculation

Values in parentheses refer to the highest resolution bin